

Ablation of ice and heat balance on Soler Glacier, Patagonia

Hiroshi Fukami¹ and Renji Naruse²

1 Geological Survey of Hokkaido, Kita 19 Nishi 12, Kita-ku, Sapporo 060 Japan

2 Institute of Low Temperature Science, Hokkaido University, Kita-ku, Sapporo 060 Japan

(Received December 18, 1986 ; Revised manuscript received January 22, 1987)

Abstract

Measurements of ablation and heat balance were made on Soler Glacier, eastern side of the Northern Patagonia Icefield, from late October to early December, 1985. Ablation of ice differed according to the surface condition. Ablation in the debris-covered zone was about twice that in the bare ice zone, owing to the difference in surface albedo. Heat balance observations were made on the bare ice zone in two periods: the small ablation period and large ablation period. The different contributions of heat balance components were obtained in these period.

1. Introduction

Measurements of ice ablation and heat balance were made on Soler Glacier, eastern side of the Northern Patagonia Icefield, as part of a hydrological and meteorological study in this region. The main ablation area, almost flat, is about 7 km long from the glacier terminus to the base of the icefalls and about 1.5 km in mean width. About 50 % of the ice surface is covered by debris. Practically all the ablation take place at the surface by means of ice melting on Soler Glacier.

Naruse and Endo (1967) made preliminary measurements of ablation on Soler Glacier in short period. Kobayashi and Saito (1985a, 1985b) did ablation and heat balance studies on the glacier, but could not accomplish the systematical measurement of ablation and radiation.

The purpose of this study was to obtain more precise data of ablation and heat balance components on the glacier. As a result, we found a clear difference in ablation between debris-covered and bare ice surface, and the characteristics of heat balance components.

2. Observation period and instrumentation

Measurements were made on the ablation area of Soler Glacier. The measurement sites are shown in Fig. 1.

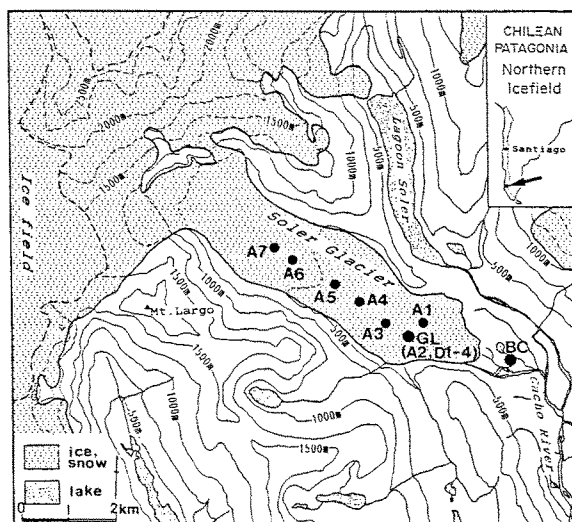


Fig. 1. Location map.

GL : meteorological measurement station and ablation measurement sites (A2, and D1-D4).

A1, A3-A7 : ablation measurement site.

BC : meteorological measurement station at terminal moraine.

Table 1. Results of ablation measurements by stake method.

| Stake name | Elevation (ma.s.l.) | Surface condition | Albedo | Observation period | Mean daily ablation (cm water) | Max. daily ablation (cm water) | Min. daily ablation (cm water) | k_w ($\frac{\text{cm}}{^{\circ}\text{C}\cdot\text{day}}$) |
|------------|---------------------|-------------------------|--------|--------------------|--------------------------------|--------------------------------|--------------------------------|---|
| A1 | ≈362 | Debris covered (type-1) | | Oct. 20-Dec. 4 | 4.4 | 7.9 | 2.1 | 0.78 |
| A2 | 378 | Bare ice | 0.44 | Oct. 20-Dec. 7 | 2.4 | 5.4 | 0.5 | 0.42 |
| A3 | 396 | Bare ice | 0.42 | Oct. 20-Dec. 4 | 2.5 | 5.7 | 0.5 | 0.44 |
| A4 | 432 | Bare ice | 0.53 | Oct. 20-Nov. 17 | 1.8 | 2.9 | 0.5 | 0.40 |
| A5 | 459 | Bare ice | 0.55 | Oct. 20-Nov. 17 | 1.8 | 3.3 | 0.1 | 0.39 |
| A6 | 514 | Bare ice | | Oct. 23-Nov. 7 | 1.6 | 3.9 | 0.5 | 0.29 |
| A7 | 535 | Bare ice | | Oct. 23-Nov. 17 | 2.2 | 4.6 | 0.8 | 0.51 |
| D1 | ≈370 | Debris covered (type-1) | 0.11 | Oct. 31-Dec. 7 | 4.3 | 7.4 | 2.0 | 0.73 |
| D2 | ≈370 | Debris covered (type-2) | 0.28 | Oct. 31-Dec. 7 | 3.4 | 5.6 | 1.2 | 0.54 |
| D3 | ≈370 | Debris covered (type-3) | 0.09 | Oct. 31-Dec. 7 | 4.3 | 8.2 | 1.6 | 0.79 |
| D4 | ≈370 | Debris covered (type-4) | 0.10 | Oct. 31-Nov. 2 | 4.4 | 9.0 | 2.3 | 0.76 |

type-1 : thin debris of small pebbles and fine sands

type-2 : patch like of fine sands

type-3 : about 1 cm thick debris of sands and small pebbles

type-4 : about 3 cm thick debris of pebbles

Ablation measurements were made by the stake method. Eleven sites were maintained at various elevations and ice surface types (Table 1). The observation period of each site is listed in Table 1.

A meteorological station was set up at GL, about 1.7 km up-glacier from the terminus, as shown in Fig. 1. The instrumentation and the results of meteorological measurements were presented by Fukami *et al.* (1987). Air temperature, humidity and wind velocity were measured during the whole period of the ablation measurement, from October 20 to December 7, 1985. The radiation measurements were carried out on the glacier from October 31 to November 6 and from November 24 to November 30. We analyzed the heat balance separately in these two periods. The former period was characterized by low air temperature and rainy weather, and the latter by high air temperature and fine weather.

3. Ablation of ice on the glacier surface

Ablation of ice was measured in the bare ice zone from A2(GL) to A7 along the center line of the glacier. Ablation measurements for different surface conditions were carried out near GL; A1, A2, and D1-D4

(see Fig. 1). Mean, minimum and maximum values of daily ablation in water equivalent at each site are listed in Table 1. The variations in the accumulated ablation amounts at all sites are shown in Fig. 2. The density of surface ice was assumed to be 850 kg/m³.

Ablation amounts at each site were roughly divided into two stages, as shown in Fig. 2; the first half

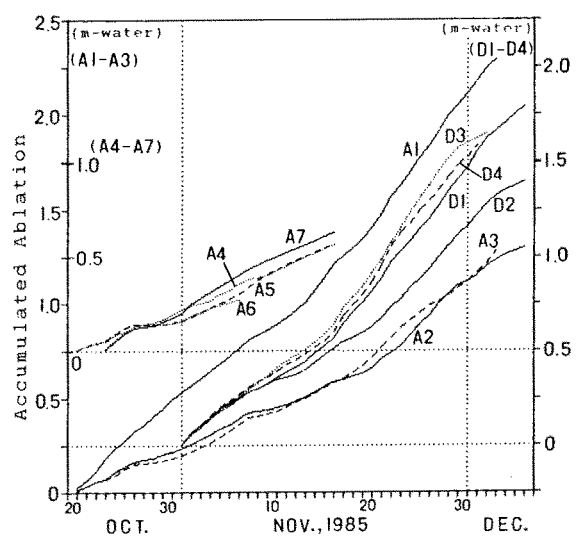


Fig. 2. Variation of accumulated ablation of each site.

was a period of small ablation rate, and the second half, that of large ablation rate. This was ascribed to the different meteorological conditions (Fukami *et al.* 1987).

In general, the accumulated ablation in water equivalent, ΣM (cm), and accumulated daily mean air temperature, ΣT ($^{\circ}\text{C} \cdot \text{day}$), are related by the following equation:

$$\Sigma M = k_w \cdot \Sigma T \quad (1)$$

where k_w is the degree day factor ($\text{cm}/^{\circ}\text{C}/\text{day}$). Two examples of the relationship between ΣM and ΣT are shown in Fig. 3, which represent good proportional relationships. The values of k_w at each site are listed in Table 1.

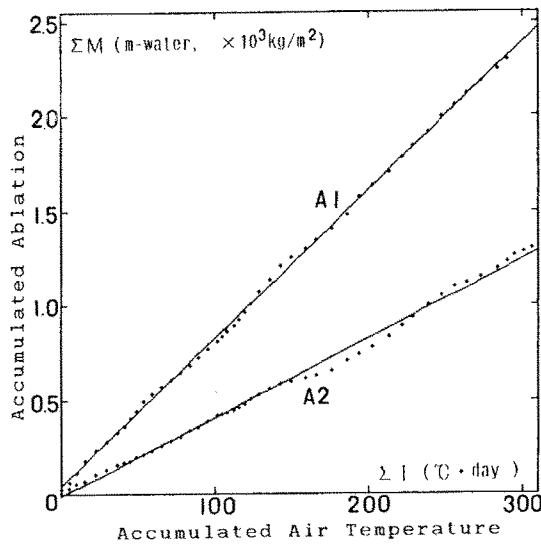


Fig. 3. Relation of accumulated ablation (ΣM) and accumulated temperature (ΣT).

The difference in ablation rate of eleven sites indicated that ablation sites could be classified into three groups of different surface conditions: 1) bare ice (A2, A3, A4, A5, A6, and A7(?)), 2) debris-covered ice (A1, D1, D3, and D4), and 3) intermediate surface (D2 and A7(?)). Ablation in the debris-covered zone was about twice that in the bare ice zone. The difference of ablation in surface condition resulted from the difference in surface albedo. However, ablation in the thick debris-covered part was smaller than in other parts. The effect of the debris thickness on the ablation rate was not clarified in our measurements, partly because of small differences in debris thickness.

There was no clear difference in surface heights between the debris-covered and the bare ice zone, in spite of the difference in the ablation rate between the

two zones. This may result from the more rapid emergence flow (an upward component of flow velocity) of ice in the debris-covered zone than in the bare ice zone, to compensate the surface lowering due to ice melting.

4. Heat balance of the glacier surface

4.1. Heat balance equation

To recognize the causes of ablation by surface ice melting, the heat balance observations were carried out at GL on the glacier. In this paper, we showed the result of heat balance observation in the bare ice zone.

As mentioned before, we analyzed about two periods: November 1-5 and November 25-29. In these periods, heat conduction to the sub-surface ice layer was zero, because ice near the surface was filled by water (0°C). Also, heat from rain was very small, compared with other heat balance components.

Therefore, the heat balance equation at the ice surface can be written as follows:

$$NR + SE + LA + QM = 0 \quad (2)$$

$$NR = SR + LR = (1 - a) S \downarrow + LR \quad (3)$$

where

NR : net radiation balance

SR : solar radiation balance

$S \downarrow$: global radiation (solar radiation)

a : albedo of ice surface

LR : long wave radiation balance

SE : sensible heat flux

LA : latent heat flux

QM : heat used for ice melting

Values of NR and SR ($S \downarrow$ and a) were measured by one net radiometer and two pyranometers. Values of SE and LA were calculated based on the supposed logarithmic profiles of air temperature, wind velocity and water vapor pressure in air. The equations used for calculation were as follows:

$$SE = \rho \cdot C_p \cdot k^2 \cdot \frac{(T_1 - T_0) \cdot U_1}{[\ln(z_1/z_0)]^2} \cdot \frac{1}{(1 + Ri)^2} \quad (4)$$

$$LA = \rho \cdot L \cdot k^2 \cdot \frac{(e_1 - e_0) \cdot U_1}{[\ln(z_1/z_0)]^2} \cdot \frac{0.622}{P} \cdot \frac{1}{(1 + Ri)^2} \quad (5)$$

$$Ri = \frac{T_m \cdot (\Delta U)^2}{g \cdot \Delta T \cdot \Delta h} \quad (6)$$

where

- ρ : density of air
- C_p : specific heat of air
- k : von Karman constant (0.4)
- T_1, T_0 : air temperature at heights z_1 and z_0
- z_1 : height of air temperature measurement (1.35 m)
- z_0 : roughness length
- L : latent heat of sublimation
- e_1, e_0 : water vapor pressure at heights z_1 and z_0
- P : atmospheric pressure
- U_1 : mean wind velocity at height z_1
- Ri : Richardson number
- g : gravitational acceleration
- ΔT : air temperature difference between z_1 and z_0
- Δh : difference between z_1 and z_0
- T_m : mean air temperature between z_1 and z_0
- ΔU : wind velocity difference between z_1 and z_0

The values of z_0 can be determined from vertical wind velocity profiles above the ice surface. To obtain the profiles, wind velocities were occasionally measured at four heights: 0.3, 0.75, 1.5, and 2.0 m. Most wind profiles were logarithmic. The mean value of z_0 was 0.0013 m. Wind velocity at height z_1 (1.35 m) was related to the wind velocity at height 1.5 m from the vertical wind profile measurements. Since the z_0 was small and ice surface was always at the melting point, T_0 and e_0 were assumed to be 0°C and

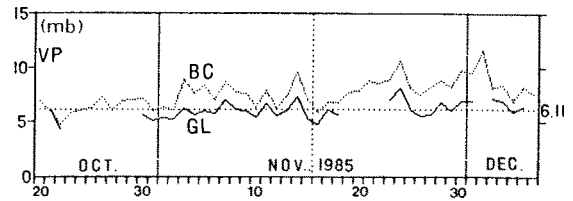


Fig. 4. Variation of daily mean vapor pressure at GL and BC.

6.11 mb respectively.

As shown in equation (5), when e_1 is smaller than 6.11 mb, LA becomes a negative heat flux; that is evaporation. The variation of the daily mean value of water vapor pressure in air is shown in Fig. 4. The vapor pressure gradually increased around 6.11 mb during the observation period.

We examined air mass stability near the ice surface using equation (6). Most hourly values of Ri were from 0.0 to 0.2, the mean value being 0.07. Air was found to be mostly in neutral or near-neutral stability. Following Weller (1968), we considered air mass stability in calculating SE and LA , as shown in equations (4) and (5).

The value of QM was derived from the surface lowering by stake measurement at A2.

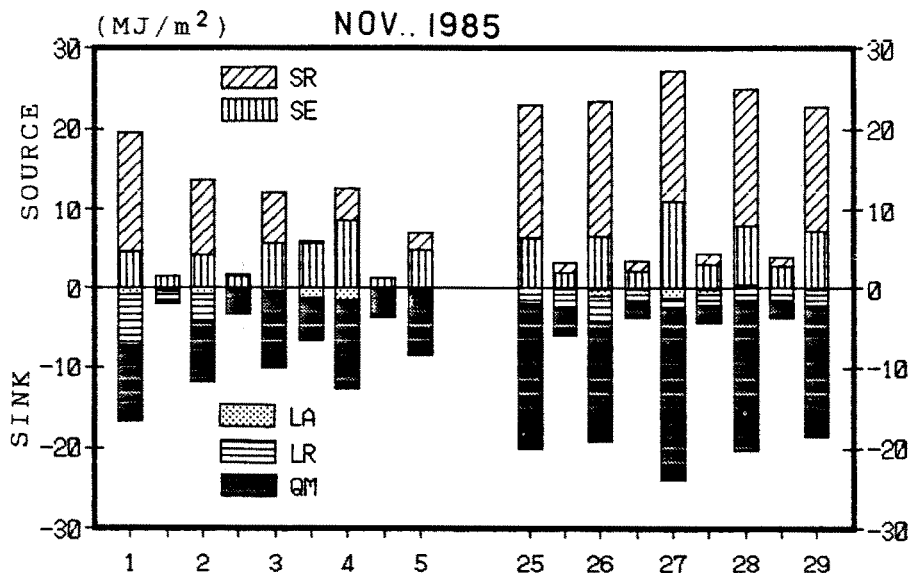


Fig. 5. Comparison of one full day (0-24hr) and night time (21-09hr) heat balance in two periods; November 1-5 and November 25-29, 1985. Night time heat balances are shown between one full day heat balances.

Table 2. Components of heat balance, Soler Glacier, November 1-5 and November 25-29, 1985.

| Period | Heat balance component | Average day time (09-21 h) | | Average night time (21-09 h) | | Average daily (24 hrs) | |
|---------------|------------------------|----------------------------|-------|------------------------------|--------|------------------------|-------|
| | | MJ/m ² | % | MJ/m ² | % | MJ/m ² | % |
| Nov. 1-5 | <i>NR</i> | 5.78 | 66 | -0.48 | -13 | 5.30 | 49 |
| | <i>(SR)</i> | (7.16) | (81) | (0.23) | (6) | (7.39) | (68) |
| | <i>(LR)</i> | (-1.38) | (-16) | (-0.71) | (-18) | (-2.09) | (-19) |
| | <i>SE</i> | 3.03 | 34 | 2.51 | 66 | 5.54 | 51 |
| | <i>LR</i> | -0.21 | -2 | -0.55 | -14 | -0.76 | -1 |
| | <i>QM</i> | -6.24 | -70 | -2.77 | -73 | -9.01 | -83 |
| | Total source | 8.81 | 100 | 2.51 | 66 | 10.84 | 100 |
| Total sink | -6.45 | -72 | -3.80 | -100 | -9.77 | -84 | |
| Nov. 25-29 | <i>NR</i> | 14.89 | 74 | -0.55 | -15 | 14.34 | 65 |
| | <i>(SR)</i> | (15.22) | (75) | (1.25) | (34) | (16.47) | (75) |
| | <i>(LR)</i> | (-0.33) | (-2) | (-1.80) | (-49) | (-2.13) | (-10) |
| | <i>SE</i> | 5.16 | 26 | 2.46 | 66 | 7.62 | 35 |
| | <i>LA</i> | 0.15 | 1 | -0.38 | -10 | -0.32 | -1 |
| | <i>QM</i> | -14.94 | -74 | -2.77 | -75 | -17.71 | -81 |
| | Total source | 20.20 | 100 | 2.46 | 66 | 21.94 | 100 |
| Total sink | -14.94 | -74 | -3.71 | -100 | -18.03 | -82 | |

4. 2. Result

The heat balance in one full day (0 hr-24 hr) and at night time (21 hr-09 hr) are shown in Fig. 5. Average values of heat balance components for the two periods are listed in Table 2. The components of the heat source and sink are also given by percentage in Table 2. Since each component was derived independently, the absolute values of the total heat source and sink did not agree. In the percentage calculation, the larger of the total source or sink was taken to be 100 %.

The difference between the two periods is seen in the heat balance components. Both the absolute values of the total heat source and sink in the latter period were larger than those in the former period; especially, solar radiation balance, *SR*, and heat of ice melting, *QM*, were large, owing to fine weather in the latter period.

Although the average long wave radiation balance, *LR*, did not differ much in the two periods (see Table 2), *LR* was a fairly large heat sink in November 1 and 2 of the former period (see Fig. 5). It was caused by the low air temperature and fine weather.

The sensible heat flux, *SE*, in the former period was smaller than that in the latter period. This can be also ascribed to the difference in air temperature between the two periods.

The latent heat flux, *LA*, was small, compared with other components, because water vapor pressure in air was close to 6.11 mb.

A Föhn-like phenomenon (Fukami *et al.*, 1987)

was recognized in the heat balance, from the night of November 3 to November 4. In this case, *SE* became large due to air temperature increase, and *LA* showed an increase in evaporation due to water vapor pressure decrease.

Under the influence of the above conditions, the average daily heat balance was different between the two periods. The total heat source in the latter period was about twice that in the former period. Although the heat source was mainly *NR* (*SR*) and *SE*, their percentages differed between the two periods. *NR* was 50 % and *SE* 50 % in the former period, while *NR* was 65 % and *SE* 35 % in the latter period. The value of *QM* in the latter period was about twice that in the former period. It is considered that these differences were produced by the fine weather in the latter period.

5. Concluding remarks

Ablation of ice was measured in the ablation area of Soler Glacier, from October 20 to December 7, 1985. Ablation became large in the latter half of the observation period, owing to the meteorological condition. Degree day factors at ablation measurement sites were obtained from the good relationship between accumulated ablation and accumulated air temperature. Ablation rate in a bare ice zone was found to be about twice that in the bare ice zone.

Heat balance of the bare ice zone was measured

in two periods: the small ablation period and large ablation period. The difference in heat balance components was obtained between the two periods. The total heat source in the large ablation period was about twice that in the small ablation period. The heat source was mainly net radiation balance (solar radiation balance) and sensible heat flux. Radiative balance was 50 % and sensible heat flux 50 % in the small ablation period, while radiative balance was 65 % and sensible heat flux 35 % in the large ablation period. Heat for ice melting in the large ablation period was about twice that in the small ablation period.

In a previous study of heat balance (Kobayashi and Saito, 1985b), the latent heat flux component was a fairly large heat source. That would be caused by the seasonal variation. Their observations were made in mid-summer in December, 1983. Considering the variation of water vapor pressure in this area (see Fig. 4), latent heat flux should become heat source (condensation) in mid-summer.

Ablation was compared with discharge of the Cacho River, which runs out from the terminus of Soler Glacier (Fukami and Escobar, 1987). It was found that the river discharge variation was closely related to the ice ablation on the glacier.

The authors measured downward all-wave radiation in the terminal moraine (BC). Using these data, the long term heat balance will be discussed in a separate paper, containing the difference of heat balance between debris-covered and bare ice.

Acknowledgments

The authors are grateful to Dr. N. Ishikawa, Institute of Low Temperature Science, Hokkaido University, for valuable comments on observation and the calculation method in the heat balance study.

References

- Fukami, H., Escobar, F., Quinteros, J., Casassa, G. and Naruse, R. (1987) : Meteorological measurements at Soler Glacier, Patagonia, in 1985. *Bulletin of Glacier Research*, **4**, 31-36.
- Fukami, H. and Escobar, F. (1987) : Hydrological characteristics of Soler Glacier drainage, Patagonia. *ibid.*, **4**, 91-96.
- Kobayashi, S. and Saito, T. (1985a) : Meteorological observations on Soler Glacier. *Glaciological Study in Patagonia Northern Icefield, 1983-1984*. Data Center for Glaciological Research, Japanese Society of Snow and Ice, 32-36.
- Kobayashi, S. and Saito, T. (1985b) : Heat balance on Soler Glacier. *ibid.*, 46-51.
- Naruse, R. and Endo, T. (1967) : Glaciological investigations of Northern Patagonian glaciers, Chile. *Seppyo*, **29**, 167-172.
- Weller, G. (1968) : The heat budget and heat transfer processes in Antarctic plateau ice and sea ice. ANARE Scientific Report, Series A(IV) Glaciology, publication No. 102, 155 p.

Resumen

Ablación de hielo y balance energético en el Glaciar Soler, Patagonia

Desde fines de Octubre a principios de Diciembre de 1985 se realizó mediciones de ablación de hielo y balance energético en la zona de ablación del Glaciar Soler, ubicado en el lado oriental del Hielo Patagónico Norte. Los lugares de medición se muestran en la Fig. 1. Para la ablación se utilizó el método de balizas en once sitios (Tabla 1). La estación meteorológica fue instalada en el sitio GL.

En la Tabla 2 se muestra una lista de valores medios, mínimos y máximos diarios de ablación en equivalente de agua para cada sitio, junto al factor día-grado, k_w (cm/°C/día). La variación de la ablación acumulada en todos los puntos se muestra en la Fig. 2. En la zona cubierta por detritos la ablación era unas dos veces mayor que aquella sobre hielo limpio. Esto se debió a la diferencia de albedo entre ambas superficies.

En la estación GL (zona de hielo limpio) se llevó a cabo observaciones de balance energético sobre el glaciar para individualizar las fuentes de calor que intervienen en el proceso de derretimiento de hielo. Se analizó durante dos períodos: del 1 al 5 de Noviembre y del 25 al 29 de Noviembre de 1985. En la Tabla 2 se muestran los valores medios de los términos del balance energético para los dos períodos. En la Fig. 5 se muestra el balance energético diario (0-24 hr) y nocturno (21-09 hr); donde NR es el balance radiativo neto, SR el balance radiativo solar, LR el balance radiativo de onda larga, SE el flujo de calor sensible, LA el flujo de calor latente y QM el calor empleado en fusión. Las fuentes totales de calor en el último período fueron unas dos veces mayor que durante el primer período. A pesar que las fuentes de calor estaban compuestas principalmente por NR (SR) y SE , su porcentaje relativo varió en los dos períodos: NR fue de 50 % y SE de 50 % en el primer período y de 65 % y 35 % respectivamente durante el segundo período.